WARSAW UNIVERSITY OF TECHNOLOGY Index 351733
FACULTY OF CIVIL ENGINEERING
COMMITTEE FOR CIVIL AND WATER ENGINEERING
POLISH ACADEMY OF SCIENCES ISSN 1230-2945

DOI: 10.24425/ace.2026.157469

ARCHIVES OF CIVIL ENGINEERING

Vol. LXXII ISSUE 1 2026

pp. 207 –222

Research paper

Study on the noise reduction characteristics of porous drainage asphalt mixes considering renewable energy

Lin Qi[1], Jiahao Liu[2], Ziang Liu[3]

Abstract: With the increasingly close connection between cities and the rapid development of large highways, this has led to the proportion of traffic noise exceeding the standard section in most cities up to 30% or more, traffic noise pollution has seriously affected people's quality of life, becoming one of the key issues of current urban pollution. In this study, for the noise reduction characteristics of porous drainage asphalt mixture, the rutting plate specimens and Marshall standard specimens with different gradation, thickness, void ratio and particle size were compared and tested by Marshall method. The test results show that the peak absorption coefficient of Porous Asphalt Concrete 13 (PAC-13) is 0.67, the average absorption coefficient is 0.3, and the noise reduction coefficient is 0.32. From the perspective of noise reduction coefficient, the value of PAC-13 is 2.46 times that of Asphalt Concrete 13(AC-13) and 1.88 times that of Stone Mastic Asphalt 13 (SMA-13). Its comprehensive noise reduction and sound absorption ability is far better than SMA-13 and AC-13. The smaller the particle size of the PAC specimen, the stronger its sound absorption capacity. The test results are in line with expectations and have some reference value for the study of urban noise pollution. The study conducted in-depth research on the noise reduction performance of commonly used asphalt materials in recent years, which provided strong support for pavement laying and urban noise reduction research.

Keywords: traffic noise, porous drainage asphalt, noise reduction characteristics, PAC-13

[1]Associate Prof., PhD., Eng., School of Materials Science and Engineering, Chang'an University, Xi'an 710064, China, e-mail: linqillqq@outlook.com, ORCID: 0009-0002-6618-8571

[2]MSc., School of Materials Science and Engineering, Chang'an University, Xi'an 710064, China, e-mail: jiahaoliu@mailn.uu.me, ORCID: 0009-0001-2158-6886

[3]MSc., School of Materials Science and Engineering, Chang'an University, Xi'an 710064, China, e-mail: zianggliu@mailn.uu.me, ORCID: 0009-0009-7046-9035

1. Introduction

Due to rapid urban construction, road traffic noise is a growing problem and about 40% of urban dwellers are exposed to severe road traffic noise, which can lead to insomnia, hearing impairment, tinnitus and immune system disorder [1–4]. Relevant studies point out that low noise thin asphalt layer is a feasible solution to alleviate road traffic noise in urban environment, which provides a quieter environment for people to live in the city [5]. At the same time, traffic noise has a great impact on social development, and areas with intensive traffic noise will have lower land prices than areas at the same level that are not affected by traffic noise, which not only affects the economic development of the area, but also has a series of negative effects [6]. Studies have shown that porous drainage asphalt mixtures can effectively reduce the noise generated by tire-pavement contact and contribute to noise pollution abatement [7]. Currently, this porous drainage asphalt pavement is widely used worldwide as a low-noise pavement [8]. Therefore, the aim of this study is to explore the noise reduction characteristics of porous drainage asphalt mixtures.

2. Related work

To promote the harmonious development of urban transportation and people's quality of life improvement, the study of noise reduction of porous drainage asphalt pavement has become a focal topic nowadays, for which researchers at home and abroad have also conducted in-depth studies. Kleizien et al. studied the effect of abrasive layer asphalt mixture composition on tire/pavement noise reduction, proposed a tire/pavement noise level prediction model based on asphalt mixture composition, and demonstrated that the noise reduction level of low-noise asphalt pavements depends on the composition of the asphalt mixture [9]. Yu T and his experimental partners considered that the asphalt aging stage plays an important role in the realization of the noise reduction and drainage function of Porous Asphalt (PA), and used molecular dynamics to simulate the contact state between water molecules and the asphalt surface layer in PA, and verified by drop observation and atomic force microscopy that different changes of interaction between aging asphalt and water molecules, the results showed that the interaction energy of asphalt and water in different aging stages is different, the longer the service life of asphalt pavement, the more severe the aging of asphalt, the greater the interaction energy with water molecules [10]. Guo et al. proposed a combination scheme of drainage surface asphalt pavement suitable for the rainfall characteristics of the Central Plains urban cluster area, systematically based on the design of pavement structure based on permeability and load-bearing capacity, the results showed that under the rainfall conditions in the region, there is no surface runoff on permeable asphalt pavement with 120 mm drainage surface layer, and it is suitable for medium traffic class of urban roads with a cumulative equivalent axle load of 10 to 12 million times, and it has enhanced both the pavement drainage and noise reduction function [11]. Zhang et al developed an indoor pavement noise reduction simulation device based on the principle of pavement noise reduction, which simulates the reflection and interference processes of noise on the surface and inside the pavement, consuming sound energy to achieve noise reduction, and the test results showed that all six asphalt mixtures used in the

study met the mechanical performance requirements [12]. Briante and his team concluded that the road pavement sound absorption depends not only on geometric and volumetric factors but also on pore shape factors. Ten porous asphalt concrete samples were tested to estimate their thickness, void fraction, sound absorption coefficient, airflow resistivity and permeability. The results confirmed the complexity of the task and indicated that estimates of pore shape factors could be derived based on the mixture volume method [13].

Tian et al. conducted a study using some powdered solid wastes as alternative fillers for asphalt mixtures, and the results showed that fly ash had a positive but insignificant effect on asphalt mixtures, porous fillers such as diatomaceous earth and red mud significantly improved the bonding properties, strength, stiffness, and aging resistance of asphalt mixtures due to their superb adsorption and hardening effect on asphalt binders, and red mud due to its intergranular pore structure [14]. The pore structure of Porous Asphalt Concrete(PAC)was evaluated by Zhu J and his team using laboratory tests and discrete element modeling simulations, where PAC specimens with different nominal maximum aggregate sizes and different gradations were prepared and tested, and the results showed that the correlation between *t*/NMAS and effective void fraction percentage was better than that of NMAS, and that disturbance size (D2.36) aggregates had a negative effect on effective void fraction, with a greater effect on smaller size mixes [15]. Manrique-Sanchez et al. considered porous friction layers as hot mix asphalt materials with high void fraction, placed as thin layers on conventional flexible pavements for safety and noise reduction benefits. The results showed that PFC layers do contribute to the structural load bearing capacity of pavements, but this contribution is highly dependent on their different microstructural and geometric characteristics [16]. Hu et al. proposed a method to design two high-viscosity modified porous asphalt mixtures with target void fractions of 20% and 22% (PAC- 10 and PAC-16) for double-layered porous asphalt pavements, including the manufacture of high-viscosity asphalt, development of aggregate gradation and optimization of asphalt aggregate ratios, and the results showed that the softening point, ductility, 60°C dynamic viscosity, rotational viscosity, complex shear modulus, phase angle and rutting coefficient of the binder were increased and the needle penetration was reduced after the addition of high-viscosity modifiers to the asphalt binder [17]. Ren et al. characterized the conventional, rheological and engineering properties of CR/SBS modified high viscosity porous asphalt binders and mixes and showed that the degree of dissolution degradation of CR significantly affects the physical and viscoelastic properties of CR/SBS modified high viscosity binders [18]. Ling and his team revealed that tire inflation noise is the main source of tire pavement noise and concluded that existing tire pavement noise measurement methods need further refinement to improve the accuracy of measurement results and that all quiet asphalt pavements have good noise reduction properties, but each has its own suitable application range [19].

Through many domestic and foreign research scholars on porous drainage asphalt and pavement noise reduction and other related aspects of in-depth research can be seen, PAC in porous drainage asphalt mixes perform well and are widely used in high-speed traffic roads in major cities. Therefore, this study on the noise reduction characteristics of PAC-13 porous drainage asphalt mixture has a certain role in promoting the study of pavement noise reduction. It provides strong theoretical support for urban pavement noise reduction and pavement economic construction.

3. Study on the design and noise testing method of porous drainage asphalt mixes considering renewable energy

3.1. Porous drainage asphalt mixture composition design

In the design of porous drainage asphalt mixture, the research uses RAP and bio-based materials as the main raw materials, which not only helps to reduce the carbon footprint of building materials, but also reduces the consumption of new resources. This design approach contributes to the goal of green building and sustainable urban development. By using recycled bitumen and other renewable materials, resource consumption in the mining and manufacturing of new materials, such as sand and other aggregates, can be reduced. This can extend the service life of natural resources and reduce the damage to the environment. The specific flow of RAP use is shown in Figure 1.

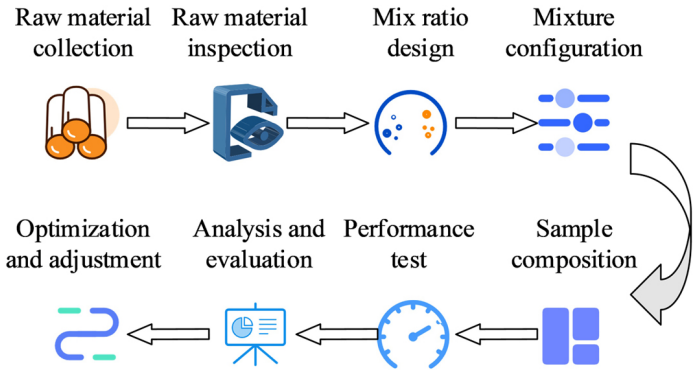

Fig. 1. RAP usage flow chart

In Figure 1, the research first collected raw materials and tested them, including water content, mix ratio and other information; Then, the mix ratio of newly added mixture was designed to prepare the mixture. After the sample is obtained, the performance test and analysis are carried out, and the sample mix ratio is optimized.

Porous drainage asphalt is a widely used pavement material that not only meets the pavement load-bearing requirements, but also has a limiting effect on the traffic noise generated by vehicles during travel [20]. The object of this study is mainly PAC-13, because the drainage and noise reduction performance of porous drainage asphalt and pavement load-bearing needs have some mutual exclusivity in the mixture void ratio, to improve the drainage and noise reduction ability of the material, the mixture needs to have a high void ratio; to improve the pavement force-bearing needs, the mixture needs to have high compactness. Therefore, finding a suitable void ratio is the main way to reach a balance between engineering and mechanical requirements. The recommended void ratio range for porous drainage asphalt mixes in China's Technical Specification for Design and Construction of Drained Asphalt Pavements is 18% to 25%. Therefore, four target void ratios were set for proportioning design in this study, which are 18%, 20%, 23% and 25%, respectively. In the gradation design of porous drainage asphalt

mixes, in addition to achieving the expected target void ratios, structural requirements are also considered to achieve a stone-rock embedded mix structure. The grading of the PAC was accomplished by adjusting the passage rate of the 2.36 mm sieve. The fine aggregates below 2.36 mm, together with the mineral powder and asphalt binding material, constituted the Maersk. 2.36 mm to 4.75 mm aggregates accounted for a small percentage and were hardly considered, while the coarse aggregates above 4.75 mm constituted the mechanical skeleton of the mix. Adjusting the passage rate of 2.36 mm sieve can effectively adjust the content of marsupial in the gap filled with coarse aggregate, and in this way the void ratio of porous drainage asphalt mix can be effectively adjusted. The preliminary grading table of PAC-13 used in this study is presented in Table 1.

Table 1. Preliminary grading table of PAC-13

Mesh size (mm)	Grading requirements			Grading 1	Grading 2	Grading 3	Grading 4	Grading 5
	Upper limit	Lower limit	Median					
16	99.9	99.9	99.9	99.9	99.9	99.9	99.9	99.9
13.2	99.9	90.1	95.2	93.5	90.9	91.4	91.4	91.2
9.5	71.2	41.3	55.6	65.4	62.4	57.1	57.1	55.1
4.75	31.1	11.3	21.2	28.5	24.7	21.8	20.8	16.3
2.36	21.3	10.1	15.6	19.3	17.4	16.5	15.6	12.9
1.18	17.1	7.2	12.3	14.2	12.9	12.3	11.7	9.8
0.6	14.3	6.1	10.1	10.9	10.1	9.7	9.3	8.2
0.3	12.4	5.2	8.6	8.1	7.7	7.5	7.3	6.8
0.15	9.3	4.3	6.6	6.8	6.8	6.3	6.3	6.2
0.075	6.2	3.1	5.1	5.5	5.5	5.2	5.2	5.2

According to the current domestic specifications, the initial asphalt dosage is calculated using the asphalt film thickness of 12 μm and the asphalt film thickness method, and the formula for estimating the asphalt dosage is shown in equation (3.1).

$$P_a = h \times C \tag{3.1}$$

In equation (3.1) h denotes the theoretical film thickness, 12 μm was used in this study, P_a denotes the mass of asphalt used as a percentage of the total mass of the asphalt mixture, i.e. the estimated amount of asphalt, and C denotes the surface area of the aggregate, which is calculated as shown in equation (3.2)

$$C = \frac{(0.41d + 0.41e + 0.82f + 1.64g + 2.87h + 6.14i + 12.29j + 32.77k)}{10^3} \tag{3.2}$$

In equation (3.2), d represents the passage rate of 19 mm sieve, e represents the passage rate of 4.75 mm sieve, f represents the passage rate of 2.36 mm sieve, g represents the passage rate of 1.18 mm sieve, h represents the passage rate of 0.6 mm sieve, i represents the passage

rate of 0.3 mm sieve, j represents the passage rate of 0.15 mm sieve and k represents the passage rate of 0.075 mm sieve. The oil to stone ratio is calculated as shown in equation (3.3).

$$P_b = \frac{P_a}{100 - P_a} \times 100 \tag{3.3}$$

In equation (3.3), P_b represents the percentage of asphalt mass to total mineral mass, i.e. oil to stone ratio. The oil-to-rock ratios for grades 1 to 5 were calculated to be 5.5, 5.3, 5.2, 5.1 and 4.8, respectively. The PAC void fraction VV was calculated with respect to the gross volume relative density γ_f and the maximum relative density γ_t, which were calculated as shown in equation (3.4).

$$VV = \left(1 - \frac{\gamma_f}{\gamma_t}\right) \times 100 \tag{3.4}$$

In equation (3.4), both the gross volume relative density γ_f and the theoretical maximum relative density γ_t are dimensionless. Among them, the measurement of the gross volume relative density is usually performed by the volumetric method or the vacuum method. Since the vacuum method will be in a vacuum state during the testing process, which may break the void structure inside the specimen and cause the void fraction to change, the void fraction is tested by the volumetric method in this study, and the test method is shown in equation (3.5).

$$\gamma_f = \frac{\rho_s}{\rho_W} \tag{3.5}$$

In the formula (3.5), ρ_w indicates the density of water at 25°, taking the value of 0.9971 g/cm^3 into, ρ_s indicates the gross bulk density of the specimen in g/cm^3, which is calculated as shown in formula (3.6).

$$\rho_s = \frac{m_l}{V} \tag{3.6}$$

In the formula (3.6), m_l indicates the measured dry mass of the specimen in g and V indicates the measured volume of the specimen. The theoretical maximum relative density γ_t is generally obtained using calculations, mainly due to the relatively high amount of asphalt in PAC, the actual measurement is relatively difficult, so the use of calculations to obtain, the calculation method is shown in equation (3.7).

$$\gamma_t = \frac{100 + P_b}{\frac{100}{\lambda_{se}} + \frac{P_b}{\lambda_m}} \tag{3.7}$$

In equation (3.7), P_b indicates the oil-to-rock ratio, λ_{se} indicates the effective relative density of the minerals, and λ_m indicates the relative density of asphalt at 25°C. In PAC, voids are generally divided into three categories: closed voids, semi-connected voids, and connected voids. Closed voids, that is, invalid voids, cannot drainage and water storage, semi-connected voids can store water, but cannot drainage, connected voids can both store water and drainage.

Connected void ratio is one of the key indicators of porous drainage asphalt, usually using the water weight method of testing, the test method is shown in equation (3.8).

$$VV' = \frac{V - V'}{V} \times 100\% \tag{3.8}$$

In equation (3.8), VV' denotes the connected void ratio of the specimen and V' denotes the closed void volume of the specimen in mm^3, which is calculated as shown in equation (3.9).

$$V' = \frac{m_l - m_w}{\rho_w} \tag{3.9}$$

In the formula (3.9), m_w denotes the mass of the specimen in water in g, ρ_w denotes the water density at room temperature, taking the value 1.0 g/cm^3. The void fraction and effective porosity of the five gradations obtained according to the above method are shown in Table 2.

Table 2. PAC-13 measured void ratio and sieve passing rate under the preliminary mix proportion

Gradation	Gradation 1	Gradation 2	Gradation 3	Gradation 4	Gradation 5
Actual void ratio (%)	18.2	19.6	21.3	25.8	25.4
Effective void ratio (%)	12.8	14.8	17.8	19.3	23.8
Passing rate of 2.36 mm sieve (%)	18.3	16.4	15.5	14.6	11.9
Passing rate of 4.75 mm sieve (%)	27.5	23.5	20.6	19.6	15.1
Difference between 4.75 mm and 2.36 mm (%)	9.3	7.7	5.7	5.3	3.3

Establishing a linear relationship between the void fraction data and the effective void fraction in Table 2, it can be found that the reliability of using the void fraction to predict the effective void fraction is 99.4%, and similarly establishing the linear relationship between the measured void fraction and the 2.36 mm sieve passage rate, 4.75 mm sieve passage rate and the linear relationship with the difference between the 2.36 mm sieve passage rate and the 4.75 mm sieve passage rate, it can be found that the correlation between them is high and exceeds 90%. According to the fitting scheme, the sieve passage rate was adjusted, and then the ore grade was changed, the specimens were made and the grade was adjusted again, and finally the specimens with the target void ratio of 18% had a 2.36 mm sieve passage rate of 18.3% and a 4.75 mm sieve passage rate of 26.2%; the specimens with a 20% void ratio had a 2.36 mm sieve passage rate of 15.5% and a 4.75 mm sieve passage rate 21.9%; for the specimen with 23% void, the 2.36 mm sieve passage rate was 13.0% and the 4.75 mm sieve passage rate was 17.0%; for the specimen with 25% void, the 2.36mm sieve passage rate was 11.4% and the 4.75 mm sieve passage rate was 13.7%. The initial asphalt dosage was calculated for the five

groups of grades, and the initial asphalt dosage was varied at a spacing of 0.6% to initialize the oil-to-rock ratio. As shown in Figure 2, the initial asphalt dosage of PAC-13 with 23% void ratio was 5.13%, and the optimum asphalt dosage was obtained between 4.63% and 4.97% in the fly-away test and the dialysis test at 4.00%, 4.50%, 5.00%, 5.50%, and 6.00%, respectively, and 4.63% was selected as the optimum asphalt dosage for PAC-13 with 23% void ratio. The optimum asphalt dosage for PAC-13 with 23% void ratio was selected.

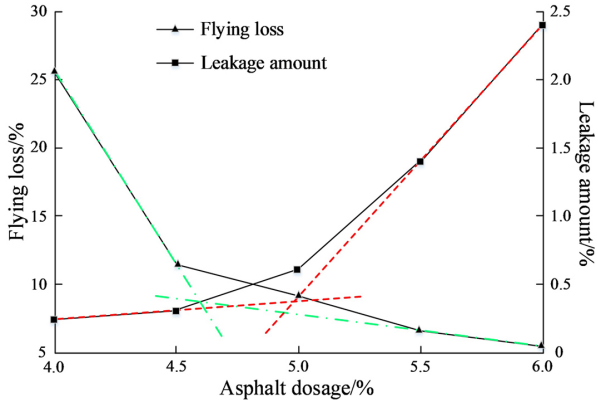

Fig. 2. The optimum asphalt dosage range of PAC-13 (VV = 23%)

Using the same method, the final optimum asphalt dosage for PAC-13 with setting target void ratios of 18%, 20%, 23% and 25% was 5.2%, 4.9%, 4.8% and 4.6%, respectively. The samples to be tested were made into standard rutting plate specimens by using rutting plate forming molds 40 × 40 × 5 cm in size and crushing them according to the reference examples in the Test Procedure for Asphalt and Asphalt Mixtures for Highway Engineering.

3.2. Road surface noise reduction analysis and noise test methods

The road noise is mainly aerodynamic noise of the car path, car engine sound and noise generated by the contact between tires and the road surface [21]. The noise generation from the tires and the road surface is shown in Figure 3.

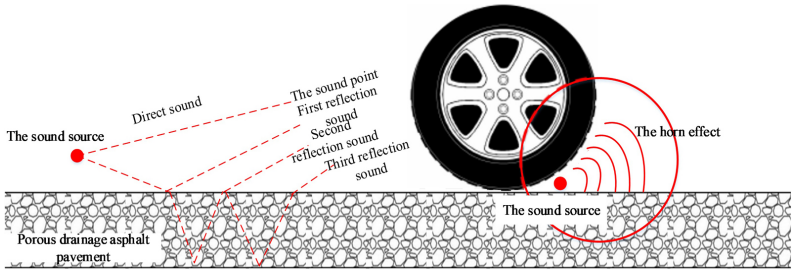

Fig. 3. Tire and ground noise propagation

Tire road noise propagating between the bottom of the car and the road surface is reflected several times, and the noise generated early on is amplified several times in the vicinity of the tire contact area of the road and its "horn effect" (the contact area can be shaped into a loudspeaker and focused on the sound of a phenomenon). The core of the noise reduction mechanism of drained asphalt pavements is their high porosity pore structure. The noise reduction effect is mainly manifested in the reduction of the propagation effectiveness of the noise generated when the tires come in contact with the road surface. Therefore, quantitative analysis and characterization of the pore structure needs to be executed for the purpose of improving the noise reduction capacity and durability of drained asphalt pavements [22]. In this study, the standing wave tube test was used to test the sound absorption performance of the specimens and used as a basis to study the noise reduction characteristics of porous drainage asphalt mixes. The circular tube transmits planar acoustic waves when the acoustic frequency f meets $f < (1.84/\pi) \cdot (C_0/D)$, as shown in Figure 4. The incident acoustic wave is emitted from the loudspeaker on the right side of the standing wave tube, and the incident wave interacts with the reflected acoustic wave on the surface of the specimen, thus forming a standing wave.

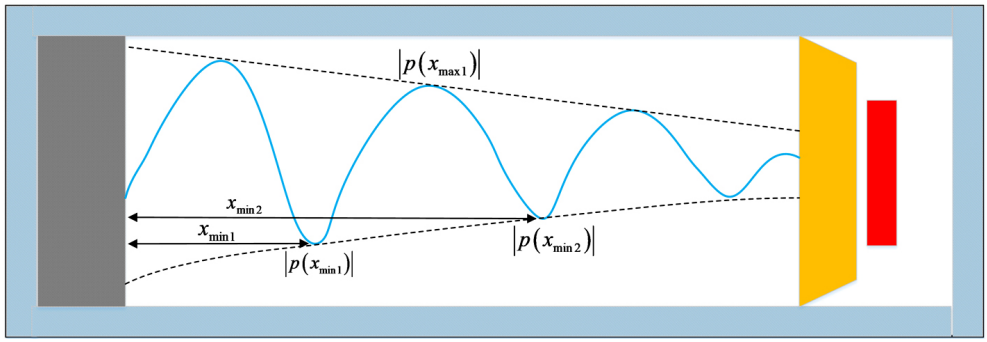

Fig. 4. Standing wave diagram of standing wave tube test

When the incident wave p_i is in phase with the reflected wave p_r, the standing wave appears as a sound pressure maximum, which is calculated as shown in equation (3.10).

$$|p_{max}| = |p_0| \cdot (1 + |r|) \tag{3.10}$$

When the incident wave p_i is reversed from the reflected wave p_r, the standing wave appears as a sound pressure minima, which is calculated as shown in equation (3.11).

$$|p_{min}| = |p_0| \cdot (1 - |r|) \tag{3.11}$$

In Eq. (3.10) and Eq. (3.11), p_0 indicates the sound pressure amplitude and r indicates the reflection factor. The absorption coefficient of the plane wave α is calculated as shown in equation (3.12).

$$\alpha = 1 - |r|^2 \tag{3.12}$$

The VSWR (Voltages Standing Wave Ratio) of s is calculated as shown in equation (3.13).

$$s = \frac{|p_{\max}|}{|p_{\min}|} = \frac{1+|r|}{1-|r|} \tag{3.13}$$

The absorption coefficient α can be calculated from the maximum and minimum values of sound pressure at that frequency, and the difference between the maximum and minimum values of sound pressure is ΔL. The standing wave ratio s and the reflection factor r are calculated as shown in equation (3.14).

$$\begin{cases} s = 10^{\Delta L/20} \\ |r| = \dfrac{s-1}{s+1} \end{cases} \tag{3.14}$$

According to equation (3.12) and equation (3.14) to obtain the final absorption coefficient α, as shown in equation (3.15).

$$ha = \frac{4 \times 10^{\Delta L/20}}{\left(10^{\Delta L/20}+1\right)^2} \tag{3.15}$$

The ability of porous drainage asphalt specimens in terms of sound absorption and noise reduction can be directly and effectively observed by looking at the spectrum of sound absorption coefficient and sound pressure level spectrum of the specimens.

4. Experiment and analysis of noise reduction characteristics of porous drainage asphalt mixes

In actual use, asphalt pavements are subject to the combined effects of different environments and traffic loads, and the service life varies without, so the degree of aging and damage varies among old roads. According to the characteristics of the waste material, a complete and detailed test and analysis report should be done first when recycling. For the design of the material composition of the recycled asphalt mixture, the most common method used today is to adjust the doping ratio of the used material to the new asphalt based on the results of the evaluation tests of the used material. The Marshall test method is used to determine the oil to stone ratio of the recycled asphalt mix. The RAP (Reclaimed Asphalt Pavement) is placed in a hot oven and heated to 125°C for a controlled time of about 3 hours. It is important to raise the temperature of the RAP material, but not so much that the old material absorbs too much heat and thus causes deterioration. Finally, the new mineral material is heated at 190–210°, and the heating and holding time is about 4 hours. When mixing the recycled material, the RAP material is mixed with the new mineral first, so that more of the old asphalt in the RAP is transferred to the new material, and then the reactive rubber asphalt is added according to the calculated dosage. The mixed recycled material was held in an oven at 145°C for 3 hours. Take 35% RAP recycled asphalt mixture as an example, the results are shown in Table 3 according to the calculated results of Marshall test.

Table 3. Technical index of Schell test of recycled asphalt mixture with 35% RAP content

Asphalt content (%)	**Bulk density ($g \cdot cm^{-3}$)**	**VV (%)**	**VMA (%)**	**VFA (%)**	**Stability (KN)**	**Flow value (0.1 mm)**
4.7	2.47	4.63	13.29	65.18	11.03	32.8
5.1	2.48	3.77	13.27	71.67	12.05	31.5
5.5	2.48	2.88	13.44	78.47	12.42	26.3
5.9	2.48	2.38	13.91	82.83	10.74	40.4
6.3	2.48	1.88	14.35	86.84	10.43	43.6

The optimum oil to stone ratio was determined to be 5.34% for the recycled material with 35% RAP old admixture. Similarly, the optimum oil to stone ratio was determined to be 5.44% and 5.24% for recycled material with 20% RAP and 50% RAP old admixture amount. The optimal asphalt admixture decreases with increasing RAP admixture, mainly because the higher the RAP admixture, the less the newly added reactive rubber asphalt. In general, due to the presence of rubber particles in rubber asphalt, its viscosity is greater such that the asphalt film on the surface of the aggregate will be thicker than that in ordinary materials. When the percentage of rubber asphalt in the total asphalt of the recycled material is reduced, the thickness of the asphalt film will also be reduced.

In this test, standing wave tube tests were conducted on Marshall specimens of different asphalt mixtures using A-weighted sound pressure levels. The sound absorption coefficients of three different grades of PAC-13, SMA-13 and AC-13 asphalt mix specimens were tested at 1/3 octave center frequencies from 100 Hz to 2000 Hz. Among them, there were 10 samples of PAC-13, SAM-13 and AC-13, and 2 samples of different thickness and porosity combinations. The test results are shown in Figure 5.

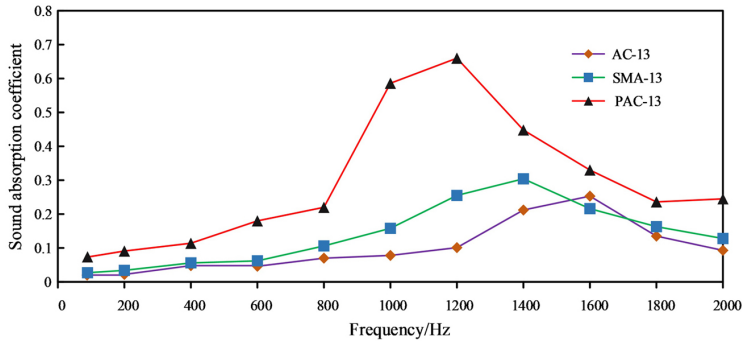

Fig. 5. Sound absorption coefficient of specimens with different frequencies

From Figure 5, the peak absorption coefficient of PAC-13 is 0.67, SMA-13 is 0.32, and AC-13 is 0.26. It can be seen that PCA-13 is far ahead of SMA-13 and AC-13 in terms of peak absorption coefficient. The absorption coefficient of PAC-13 is smaller in the low

frequency range and larger in the middle and high frequency range, which indicates that the PAC with a larger void ratio structure has a stronger absorption ability for middle and high frequency noise, which is consistent with the structural characteristics of PAC. The average absorption coefficients and noise reduction coefficients of the three grades of asphalt mixes were calculated. the average absorption coefficient of PAC-13 was 0.3 and the noise reduction coefficient was 0.32; the average absorption coefficient of SMA-13 was 0.14 and the noise reduction coefficient was 0.17; the average absorption coefficient of AC-13 was 0.1 and the noise reduction coefficient was 0.13. The value of PAC-13 is 3 times that of AC-13 and 2.14 times that of SMA-13; from the viewpoint of noise reduction coefficient, the value of PAC-13 is 2.46 times that of AC-13 and 1.88 times that of SMA-13. The test results show that the sound absorption and noise reduction performance of PAC-13 is the best among the three graded asphalt mixes, which is attributed to the characteristic of PAC-13 having high void ratio, and the noise entering the interior of the specimen will cause consumption in the void transmission, thus achieving noise reduction. To study the effect of thickness on the noise reduction characteristics of asphalt mixes, 35 mm, 45 mm, 55 mm and 65 mm were selected as the thickness variables to produce specimens of PAC-13 at four thicknesses and conduct standing wave tube tests, and the results obtained are shown in Figure 6.

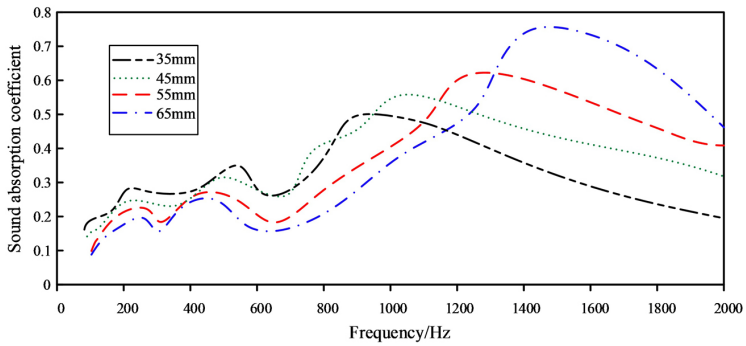

Fig. 6. Spectrum diagram of sound absorption coefficient of PAC-13 with different thickness

As can be seen from Figure 6, the influence of thickness on the sound absorption coefficient is large and the law is intuitive. The peak absorption coefficient and peak frequency become larger as the thickness of the specimen increases, and the peak absorption coefficients from 65 mm to 35 mm are 0.762, 0.617, 0.554, and 0.496, respectively; the peak frequencies are 1521 Hz, 1342 Hz, 1076 Hz, and 934 Hz respectively, which will be better. However, this does not mean that thicker pavement should be paved in one-sided pursuit of noise reduction performance, but also needs to be considered with the actual situation of the project and economic factors. Therefore, it is not advisable to increase the thickness to improve the sound and noise absorption of the pavement.

The void ratio also has an important influence on the noise reduction function of asphalt mixture. Simulating the noise generated by tires and road surface at different speeds, the average noise sound pressure level of PAC-13 with void ratio of 18%, 20%, 23% and 25% were tested, and the test results obtained are shown in Figure 7.

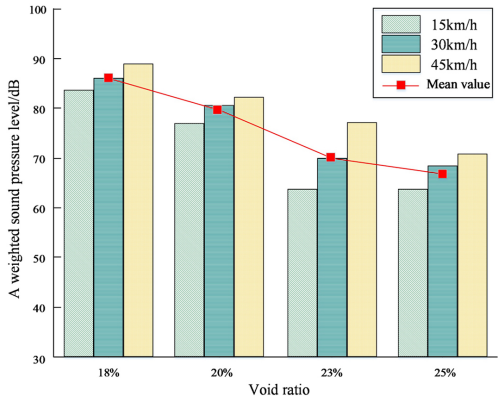

Fig. 7. Average noise sound pressure level of PAC-13

As shown in Figure 7, the comparison of noise data with different void ratios shows that the sound pressure level becomes smaller as the void ratio increases, and from the average sound pressure level, the average sound pressure level of PAC-13 with 18%, 20%, 23% and 25% void ratios are 85.8 dB, 80.3 dB, 72.3 dB and 67.5 dB, respectively. It can be seen from the four sets of data that for every 2% increase in void ratio, the noise SPL decreases by 3–6 dB, indicating that the void ratio has a significant effect on pavement noise reduction. This is because the high porosity PAC samples have more connected pores, which provides more time and space to convert sound energy into heat, which is consumed when the noise factor is transmitted to the pavement. In addition, the macrostructure of the surface of the high porosity PAC specimen is relatively larger, and the contact area between the tire and the porous asphalt specimen surface is then relatively reduced, so the noise reduction capability of the high porosity specimen will be stronger. The interaction of the two makes the larger porosity more beneficial to reduce road noise. To observe the effect of different particle sizes on the sound absorption coefficient and compare the sound absorption performance of PAC specimens with different particle sizes under the same porosity, PAC-13 specimens with 18% and 23% porosity were tested with PAC-10 specimens with 18% and 23% porosity, and the test results obtained are shown in Figure 8.

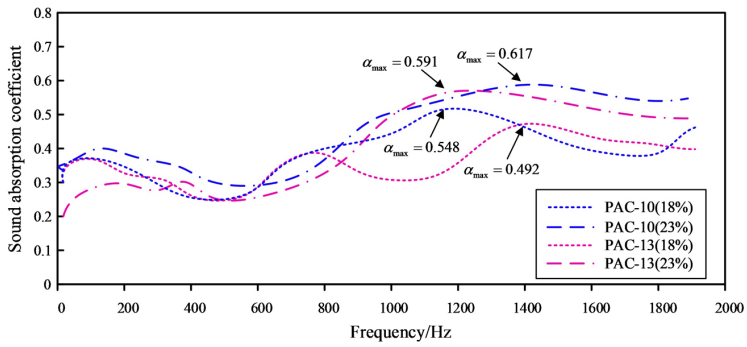

Fig. 8. Spectrum diagram of acoustic absorption coefficient of PAC with different particle sizes

As can be seen from Figure 8, the absorption coefficient curve of PAC-10 is higher than that of PAC-13 at the same void ratio, which indicates that the PAC with small particle size has a stronger absorption capacity. Because the internal structure of small particle size PAC will be more precise and proportional, the internal communication gap is also smaller compared with large particle size PAC. When the sound from the standing wave tube speaker is perpendicular to the surface of the specimen, the sound that can enter the specimen will be more, and the probability of sound diffraction and absorption is stronger in the small communication path, so the sound energy reflected and transmitted to the end of the standing wave tube will become less, and the sound energy measured by the sensor will be less, therefore, the sound absorption coefficient calculated by the small particle size PAC is greater than that of the large particle size PAC.

5. Conclusions

In this study, for the noise reduction characteristics of porous drainage asphalt mixes, the Marshall method was used to make rutting plate specimens and Marshall standard specimens to conduct comparative tests on asphalt mixes with different gradations, thicknesses, void ratios and particle sizes. The test results showed that the peak absorption coefficient of PAC-13 was 0.67, the average absorption coefficient was 0.3, and the noise reduction coefficient was 0.32. From the perspective of noise reduction coefficient, the value of PAC-13 is 2.46 times that of AC-13 and 1.88 times that of SMA-13. Its comprehensive noise reduction and sound absorption ability is far better than SMA-13 and AC-13. In the test of PAC-13 with different thicknesses, it was found that the peak absorption coefficient and peak frequency became larger when the thickness of the specimens became larger. In the tests of PAC-13 specimens with different void ratios, it was found that the sound pressure level of noise increased by 3–6 dB for every 2% decrease in the void ratio of the specimens, and in the tests of PAC specimens with different particle sizes, it was found that the smaller the particle size of PAC, the stronger its sound absorption capacity. The above test results are in accordance with the structural principle of PAC and meet the test expectations. There are some shortcomings in this study, for example, the number of specimens used in the test is not enough, and the thickness, void ratio and particle size of different graded specimens are not studied in depth. It is expected that in future studies, more specimens can be made to study more comprehensively the effects of different properties on the noise reduction characteristics of porous drainage asphalt mixtures to improve the accuracy of the test. The study conducted in-depth research on the noise reduction performance of commonly used asphalt materials in recent years, which provided strong support for pavement laying and urban noise reduction research.

Funding

The research is supported by: the National Natural Science Foundation of China (Grant No. 51908058).

References

[1] C. Gao, K. Eunyoung, G.M. Zhao, and S. Gao, "Analysis of the impact of the urban traffic noise on the vertical distribution of high-rise residential buildings", *IOP Conference Series: Earth and Environmental Science*, vol. 831, art. no. 012080, 2021, doi: 10.1088/1755-1315/831/1/012080.

[2] M. Li and J. Liu, "A Microscopic Prediction Model for Traffic Noise in Adjacent Regions to Arterial Roads", *Archives of Acoustics*, vol. 48, no. 3, pp. 433–449, 2023, doi: 10.24425/aoa.2023.145238.

[3] M. Hałucha, J. Bohatkiewicz, and P. Mioduszewski, "Modeling the effect of electric vehicles on noise levels in the vicinity of rural road sections", *Archives of Civil Engineering*, vol. 69, no. 3, pp. 573–586, 2023, doi: 10.24425/ace.2023.146098.

[4] W. Batko, L. Radziszewski, and A. Bąkowski, "A Scalar Measure of Acoustic Hazard Assessment", *Archives of Acoustics*, vol. 49, no. 3, pp. 299–306, 2024, doi: 10.24425/aoa.2024.148793.

[5] A. Grangeiro de Barros, J.K. Kampen, and C. Vuye, "The Impact of Thin Asphalt Layers as a Road Traffic Noise Intervention in an Urban Environment", *Sustainability*, vol. 13, no. 22, art. no. 12561, 2021, doi: 10.3390/su132212561.

[6] A. Bąkowski and L. Radziszewski, "Measurements of urban traffic parameters before and after road reconstruction", *Open Engineering*, vol. 11, no. 1, pp. 365–376, 2021, doi: 10.1515/eng-2021-0035.

[7] L. Al Khateeb, K. Anupam, S. Erkens, and T. Scarpas, "Micromechanical simulation of porous asphalt mixture compaction using discrete element method (DEM)", *Construction and Building Materials*, vol. 301, no. 1, art. no. 124305, 2021, doi: 10.1016/j.conbuildmat.2021.124305.

[8] W. Luo and L. Lim, "Development of a new analytical water film depth (WFD) prediction model for asphalt pavement drainage evaluation", *Construction and Building Materials*, vol. 218, pp. 530–542, 2019, doi: 10.1016/j.conbuildmat.2019.05.142.

[9] R. Kleiziene, O. Sernas, A. Vaitkus, and R. Simanaviciene, "Asphalt Pavement Acoustic Performance Model", *Sustainability*, vol. 11, no. 10, art. no. 2938, 2019, doi: 10.3390/su11102938.

[10] T. Yu, H. Zhang, and Y. Wang, "Interaction of asphalt and water between porous asphalt pavement voids with different aging stage and its significance to drainage", *Construction and Building Materials*, vol. 252, art. no. 119085, 2020, doi: 10.1016/j.conbuildmat.2020.119085.

[11] X. Guo, J. Zhang, B. Zhou, W. Liu, J. Pei, and Y. Guan ,"Sponge roads: The permeable asphalt pavement structures based on rainfall characteristics in central plains urban agglomeration of China", *Water Science & Technology*, vol. 80, no. 9, pp. 1740–1750, 2019, doi: 10.2166/wst.2019.426.

[12] H. Zhang, Z. Liu, and X. Meng, "Noise reduction characteristics of asphalt pavement based on indoor simulation tests", *Construction and Building Materials*, vol. 215, pp. 285–297, 2019, doi: 10.1016/j.conbuildmat.2019.04.220.

[13] F.G. Praticò, R. Fedele, and P.G. Briante, "On the Dependence of Acoustic Pore Shape Factors on Porous Asphalt Volumetrics", *Sustainability*, vol. 13, no. 20, art. no. 11541, 2021, doi: 10.3390/su132011541.

[14] Y. Tian et al., "Laboratory investigation on effects of solid waste filler on mechanical properties of porous asphalt mixture", *Construction and Building Materials*, vol. 279, art. no. 122436, 2021, doi: 10.1016/j.conbuildmat.2021.122436.

[15] J. Zhu, T. Ma, Z. Lin, J. Xu, and X. Qiu, "Evaluation of Internal Pore Structure of Porous Asphalt Concrete based on Laboratory Testing and Discrete-Element Modeling", *Construction and Building Materials*, vol. 273, art. no. 121754, 2020, doi: 10.1016/j.conbuildmat.2020.121754.

[16] L. Manrique-Sanchez and S. Caro, "Numerical assessment of the structural contribution of porous friction courses (PFC)", *Construction and Building Materials*, vol. 225, pp. 754–764, 2019, doi: 10.1016/j.conbuildmat.2019.07.200.

[17] J. Hu, T. Ma, Y. Zhu, X. Huang, J. Xu, and L. Chen, "High-viscosity modified asphalt mixtures for double-layer porous asphalt pavement: design optimization and evaluation metrics", *Construction and Building Materials*, vol. 271, art. no. 121893, 2021, doi: 10.1016/j.conbuildmat.2020.121893.

[18] S. Ren, X. Liu, J. Xu, and P. Lin, "Investigating the role of swelling-degradation degree of crumb rubber on CR/SBS modified porous asphalt binder and mixture", *Construction and Building Materials*, vol. 300, art. no. 124048, 2021, doi: 10.1016/j.conbuildmat.2021.124048.

[19] S. Ling, F. Yu, D. Sun, G. Sun, and L. Xu, "A comprehensive review of tire-pavement noise: generation mechanism, measurement methods, and quiet asphalt pavement", *Journal of Cleaner Production*, vol. 287, art. no. 125056, 2020, doi: 10.1016/j.jclepro.2020.125056.

[20] F.G. Praticò, P.G. Briante, G. Colicchio, and R. Fedele, "An experimental method to design porous asphalts to account for surface requirements", *Journal of Traffic and Transportation Engineering (English Edition)*, vol. 8, no. 3, pp. 439–452, 2020, doi: 10.1016/j.jtte.2019.05.006.

[21] H. Heo, M. Sofield, J. Ju, and A. Neogi, "Acoustic Metasurface-Aided Broadband Noise Reduction in Automobile Induced by Tire-Pavement Interaction", *Materials*, vol. 14, no. 15, art. no. 4262, 2021, doi: 10.3390/ma14154262.

[22] M.A. Azadgoleh, et al., "Characterization of contaminant leaching from asphalt pavements: a critical review of measurement methods, reclaimed asphalt pavement, porous asphalt, and waste-modified asphalt mixtures", *Water Research*, vol. 219, art. no. 118584, 2022, doi: 10.1016/j.watres.2022.118584.

Received: 2024-05-09, Revised: 2024-09-02